# Supporting Information

## Morphology Controlled Growth of Crystalline Ag-Pt Alloyed Shells onto Au Nanotriangles and their Plasmonic Properties

*Xiaobin Xie,*[†‡] *Marijn A. van Huis,*[†] *and Alfons van Blaaderen*[*†‡]

† Soft Condensed Matter, Debye Institute for Nanomaterials Science, Utrecht University, Princetonplein 5, 3584 CC Utrecht, the Netherlands

‡ Present Address: Analytical & Testing Center, Sichuan University, Chengdu 610064, China

* Corresponding Author:

X. Xie E-mail: xb.xie@hotmail.com; A. van Blaaderen E-mail: A.vanBlaaderen@uu.nl.

**Contents**

## 1 Determination of Au NTs concentration

Determination of the concentration of Au NTs stock solution. The concentration of Au NTs solution was calculated by measuring the UV-VIS spectra and the equations showed as follow.[S1]

$$\varepsilon = 1.6888 \times 10^{8} e^{5.1742 \times 10^{-3} \times \lambda_{max}} \qquad (1)$$

$$C = \frac{A}{\varepsilon l} \qquad (2)$$

Where ε is extinction coefficient, $\lambda_{max}$ is the wavelength of LSPR band of Au NTs, and A is the extinction intensity.

## 2 Reactions conditions of synthesis

### 2.1 Synthesis of Au NT-AgPt NPs

**Table S1.** The reaction conditions used for Au NT-AgPt NPs growth

| | Au NT Solution | De-ionized Water | 0.1 M CTAC | 10 mM $AgNO_3$ | 10 mM $K_2PtCl_4$ | 0.10 M AA | Figure |
|---|---|---|---|---|---|---|---|
| **1** | 1.50 mL | 7.30 mL | 1.00 mL | 50 μL | 50 μL | 100 μL | Fig. 1 |
| **2** | 1.50 mL | 7.30 mL | 1.00 mL | 60 μL | 50 μL | 100 μL | Fig. 2a |
| **3** | 1.50 mL | 7.30 mL | 1.00 mL | 50 μL | 50 μL | 100 μL | Fig. 2b |
| **4** | 1.50 mL | 7.30 mL | 1.00 mL | 40 μL | 50 μL | 100 μL | Fig. 2c |
| **5** | 1.50 mL | 7.30 mL | 1.00 mL | 30 μL | 50 μL | 100 μL | Fig. 2d |
| **6** | 1.50 mL | 7.30 mL | 1.00 mL | 20 μL | 50 μL | 100 μL | Fig. 2e |
| **7** | 1.50 mL | 7.30 mL | 1.00 mL | 10 μL | 50 μL | 100 μL | Fig. 2f |
| **8** | 1.00 mL | 7.80 mL | 1.00 mL | 50 μL | 50 μL | 100 μL | Fig. S3a |
| **9** | 1.50 mL | 7.30 mL | 1.00 mL | 50 μL | 50 μL | 100 μL | Fig. S3b |
| **10** | 2.00 mL | 6.80 mL | 1.00 mL | 50 μL | 50 μL | 100 μL | Fig. S3c |
| **11** | 3.00 mL | 5.80 mL | 1.00 mL | 50 μL | 50 μL | 100 μL | Fig. S3d |
| **12** | 1.50 mL | 7.50 mL | 1.00 mL | 10 μL | 10 μL | 20 μL | Fig. S8a |
| **13** | 1.50 mL | 7.50 mL | 1.00 mL | 5.0 μL | 10 μL | 20 μL | Fig. S8b |
| **14** | 1.50 mL | 7.50 mL | 1.00 mL | 2.5 μL | 10 μL | 20 μL | Fig. S8c |
| **15** | 1.50 mL | 7.50 mL | 1.00 mL | 1.0 μL | 10 μL | 20 μL | Fig. S8d |
| **16** | 1.50 mL | 7.30 mL | 1.00 mL | 60 μL | / | 100 μL | Fig. S4a |
| **17** | 1.50 mL | 7.30 mL | 1.00 mL | 10 μL | 50 μL | 100 μL | Fig. S4b |
| **18** | 1.50 mL | 7.30 mL | 1.00 mL | 10 μL | 20 μL | 100 μL | Fig. S4c |

| | | | | | | | |
|---|---|---|---|---|---|---|---|
| **19** | 1.50 mL | 7.30 mL | 1.00 mL | / | 50 μL | 100 μL | Fig. S4d, Fig. S5 |
| **20** | 1.50 mL | 7.30 mL | 1.00 mL | 50 μL | 50 μL | 100 μL | Fig. S6a |
| **21** | 1.50 mL | 7.30 mL | 1.00 mL | 50 μL | 40 μL | 100 μL | Fig. S6b |
| **22** | 1.50 mL | 7.30 mL | 1.00 mL | 50 μL | 30 μL | 100 μL | Fig. S6c |
| **23** | 1.50 mL | 7.30 mL | 1.00 mL | 50 μL | 20 μL | 100 μL | Fig. S6d |
| **24** | 1.50 mL | 7.00 mL | 1.00 mL | 50 μL | 50 μL | 500 μL | Fig. S9a |
| **25** | 1.50 mL | 7.40 mL | 1.00 mL | 50 μL | 50 μL | 100 μL | Fig. S9b |
| **26** | 1.50 mL | 7.40 mL | 1.00 mL | 50 μL | 50 μL | 40 μL | Fig. S9c |
| **27** | 1.50 mL | 7.40 mL | 1.00 mL | 50 μL | 50 μL | 20 μL | Fig. S9d |

### 2.2 Synthesis of Au NT-AgPt NPs with adding KI

**Table S2.** The reaction conditions used for Au NT-AgPt NPs growth.

| | **Au NT Solution** | **De-ionized Water** | **0.1 M CTAC** | **10 mM KI** | **10 mM $AgNO_3$** | **10 mM $K_2PtCl_4$** | **0.10 M AA** | **Figure** |
|---|---|---|---|---|---|---|---|---|
| **1** | 1.50 mL | 7.40 mL | 1.00 mL | 60 μL | 10 μL | 20 μL | 100 μL | Fig. S10a |
| **2** | 1.50 mL | 7.40 mL | 1.00 mL | 30 μL | 10 μL | 20 μL | 100 μL | Fig. S10b |
| **3** | 1.50 mL | 7.40 mL | 1.00 mL | 15 μL | 10 μL | 20 μL | 100 μL | Fig. S10c |
| **4** | 1.50 mL | 7.40 mL | 1.00 mL | 10 μL | 10 μL | 20 μL | 100 μL | Fig. S10d |
| **5** | 1.50 mL | 7.40 mL | 1.00 mL | 5 μL | 10 μL | 20 μL | 100 μL | Fig. S10e |
| **6** | 1.50 mL | 7.40 mL | 1.00 mL | / | 10 μL | 20 μL | 100 μL | Fig. S10f |

### 2.3 Synthesis of Au NT-AuAgPt NPs

**Table S3.** The reaction conditions used for Au NT-AuAgPt NPs growth.

| | **Au NT Solution** | **De-ionized Water** | **0.1 M CTAC** | **10 mM $HAuCl_4$** | **10 mM $AgNO_3$** | **10 mM $K_2PtCl_4$** | **0.10 M AA** | **Figure** |
|---|---|---|---|---|---|---|---|---|
| **1** | 1.50 mL | 7.40 mL | 1.00 mL | 40 μL | 20 μL | 30 μL | 100 μL | Fig. S14 a, e, m |
| **2** | 1.50 mL | 7.40 mL | 1.00 mL | 30 μL | 30 μL | 30 μL | 100 μL | Fig. S14 b, f, n |
| **3** | 1.50 mL | 7.40 mL | 1.00 mL | 20 μL | 40 μL | 30 μL | 100 μL | Fig. S14 c, g, o |
| **4** | 1.50 mL | 7.40 mL | 1.00 mL | 10 μL | 50 μL | 30 μL | 100 μL | Fig. S14 d, h, p |

### 2.4 Synthesis of Au NT-AgPd NPs

**Table S4.** The reaction conditions used for Au NT-AgPd NPs growth.

| | Au NT Solution | De-ionized Water | 10 mM $AgNO_3$ | 10 mM $Na_2PdCl_4$ | 0.10 M AA | Figure |
|---|---|---|---|---|---|---|
| **1** | 2.50 mL | 7.40 mL | / | 50 µL | 100 µL | Fig. S15a |
| **2** | 2.50 mL | 7.40 mL | 10 µL | 40 µL | 100 µL | Fig. S15b |
| **3** | 2.50 mL | 7.40 mL | 20 µL | 30 µL | 100 µL | Fig. S15c |
| **4** | 2.50 mL | 7.40 mL | 30 µL | 20 µL | 100 µL | Fig. S15d |
| **5** | 2.50 mL | 7.40 mL | 40 µL | 10 µL | 100 µL | Fig. S15e |
| **6** | 2.50 mL | 7.40 mL | 50 µL | / | 100 µL | Fig. S15f |

### 3 Key physical parameters of bulk Au, Ag, Pd, and Pt

A number of physical parameters of Au, Ag, Pd, and Pt are summarized in Table S4, which include their lattice parameters, and the standard reduction potentials.[S2-S5]

**Table S5.** Key physical parameters of Au, Ag, Pd, and Pt

| | Au | Ag | Pd | Pt |
|---|---|---|---|---|
| **Lattice Parameters** | 4.078 Å | 4.086 Å | 3.891 Å | 3.924 Å |
| **Atomic Radius** | 1.442 Å | 1.444 Å | 1.376 Å | 1.387 Å |
| **Standard Reduction Potentials (V)** | +1.00 ($[AuCl_4]^-$) | +0.80 ($Ag^+$) | +0.59 ($[PdCl_4]^{2-}$) | +0.76 ($[PtCl_4]^{2-}$) |

## 4 Supporting Figures

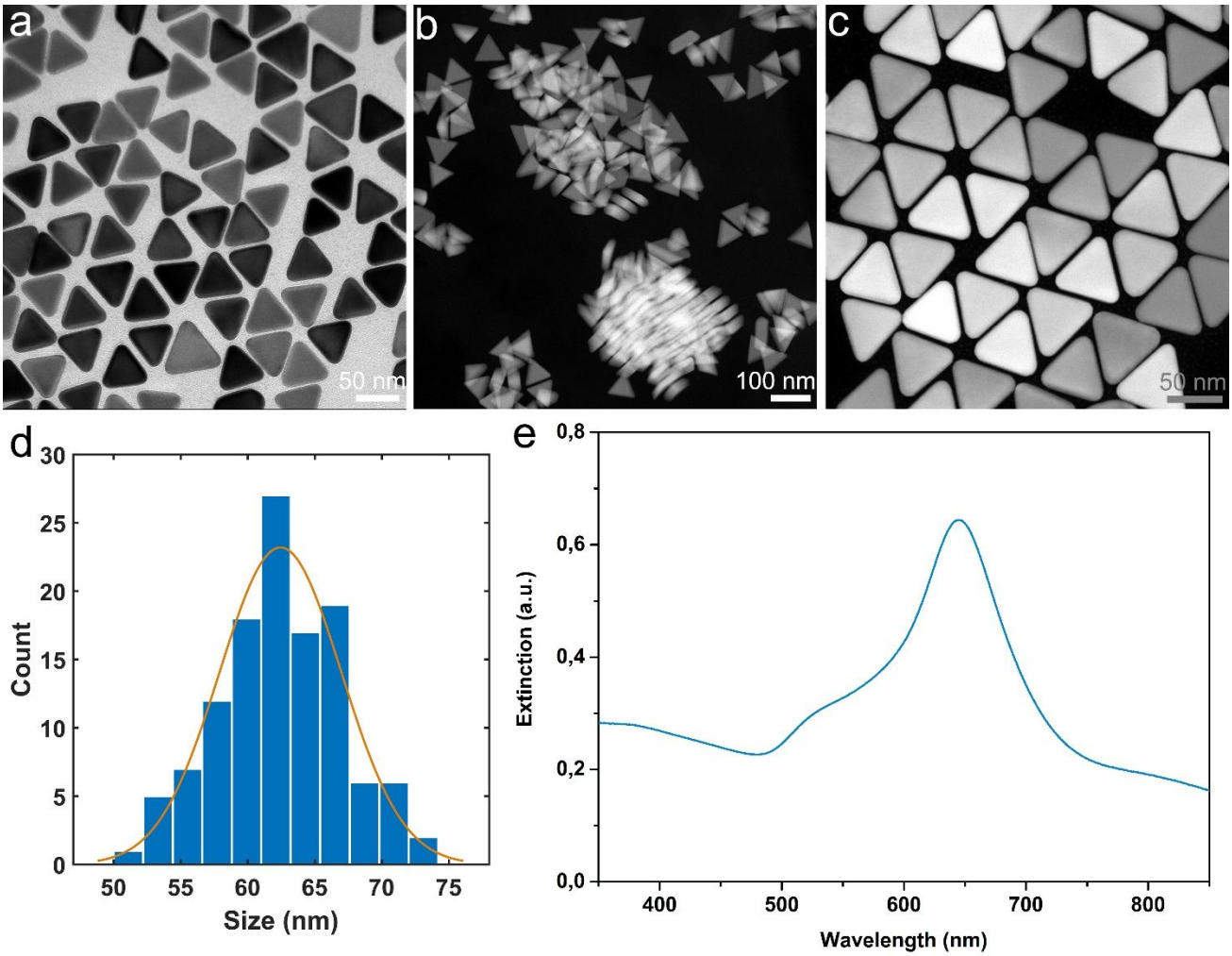


**Figure S1.** Morphology, size, and main localized surface plasmon resonance (LSPR) band of Au NTs. a) bright-field TEM image of Au NTs; b & c) HAADF-STEM images of Au NTs; d) histogram of edge length of Au NTs; e) UV-VIS spectrum of Au NTs.

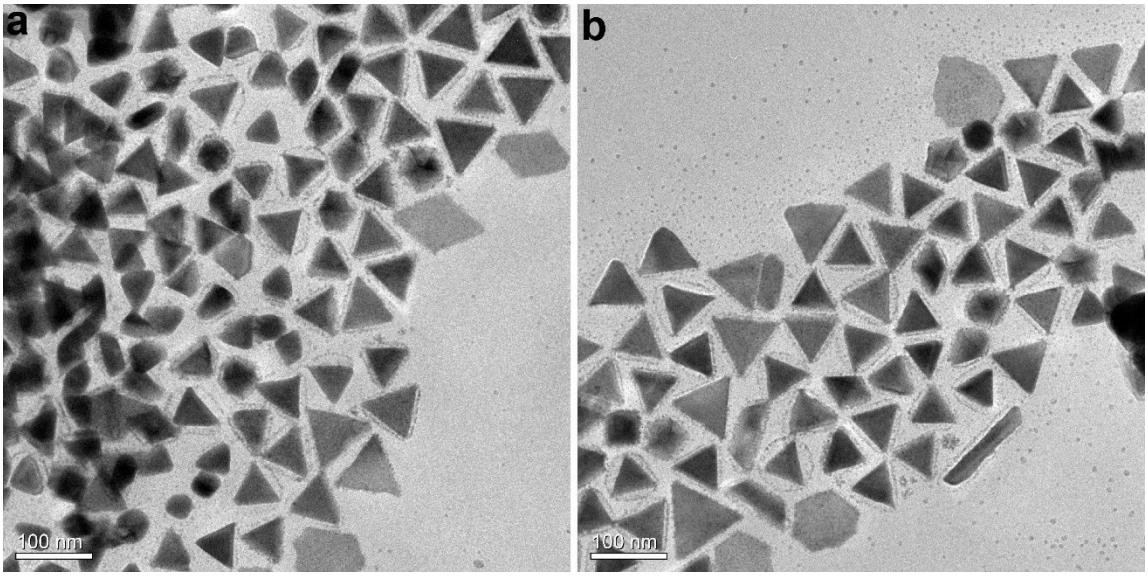


**Figure S2.** Structural stability of Au NT-AgPt yolk-shell NPs. TEM images of Au NT-AgPt yolk-shell NPs which were placed on a TEM grid for more than six years. The Au NT-AgPt yolk-shell NPs were synthesized and dropped on the TEM grid in September 2016, TEM images showed here were acquired in June 2023. The original morphology of these Au NT-AgPt yolk-shell NPs are showed in Figure 1.

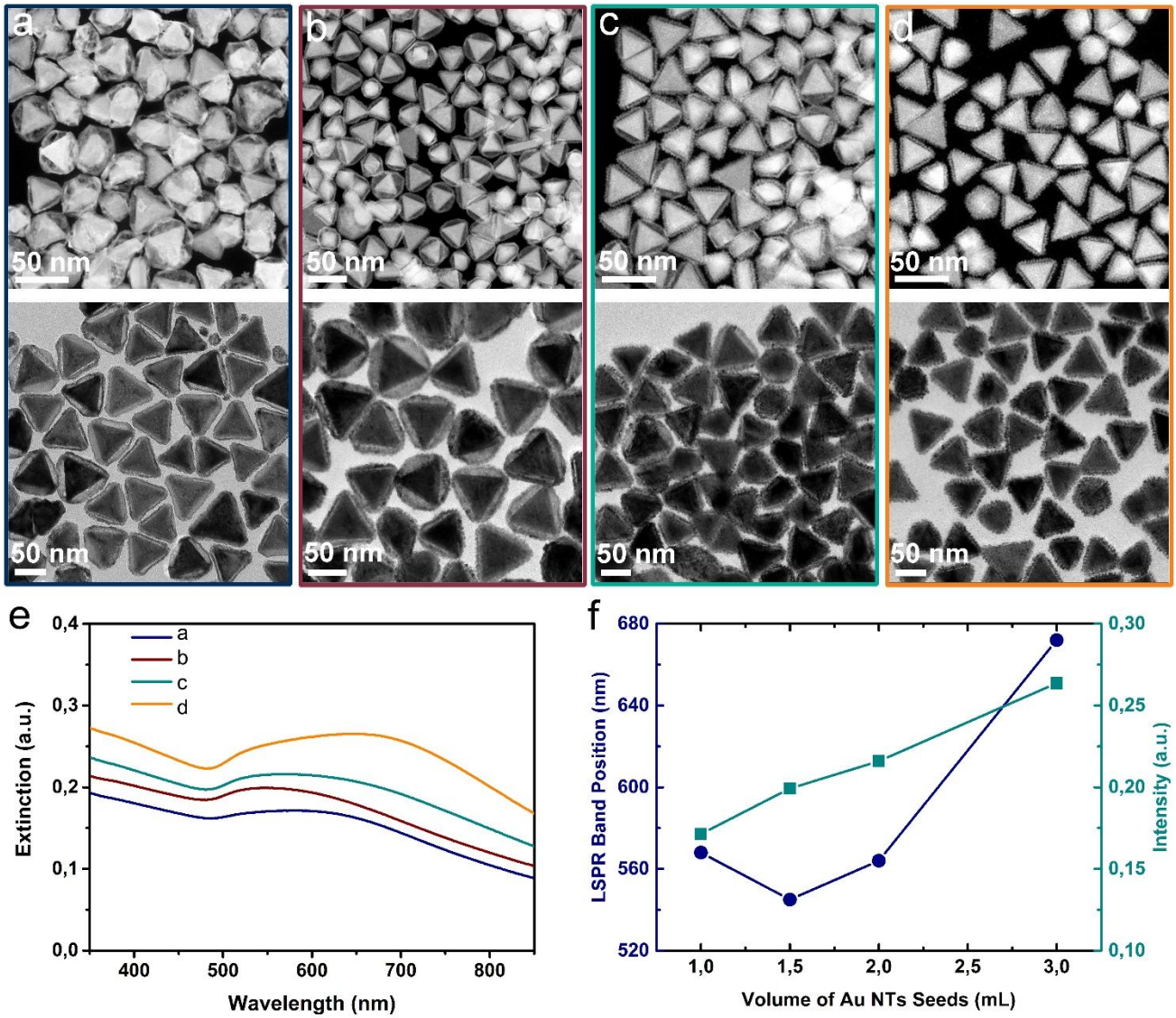


**Figure S3.** Morphological evolution of Au NT-AgPt NPs synthesized with various concentrations of Au NTs. STEM-HAADF (up) and TEM (down) images indicated Au NT-AgPt NPs acquired as the volume of Au NTs was: a) 1.0 mL, b) 1.5 mL, c) 2.0 mL, d) 3.0 mL. e) UV-Vis spectra and f) LSPR band position of Au NT-AgPt NPs showed in a-d. More details of the synthesis are shown in Table S1.

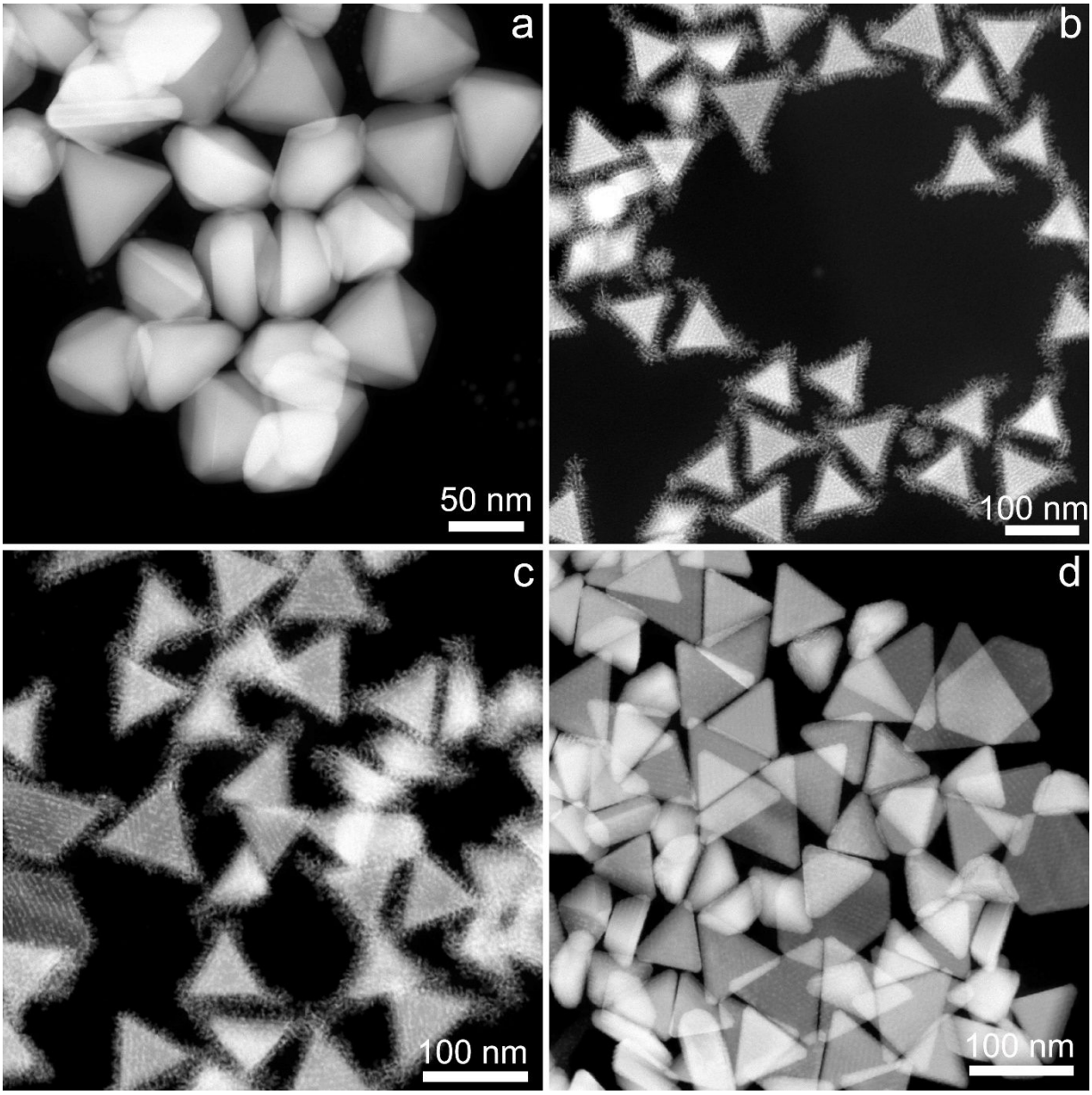


**Figure S4.** Shape evolution of Au NT-AgPt NPs synthesized by using different $AgNO_3$ and $K_2PtCl_4$ ratios. STEM-HAADF images indicated NPs acquired as the concentration of $AgNO_3$ and $K_2PtCl_4$ ratios in the growth solution was: (a) $AgNO_3$ (60 μM)/ $K_2PtCl_4$ (0 μM), (b) $AgNO_3$ (10 μM)/ $K_2PtCl_4$ (50 μM), (c) $AgNO_3$ (10 μM)/ $K_2PtCl_4$ (20 μM), and (d) $AgNO_3$ (0 μM)/ $K_2PtCl_4$ (50 μM). More details of the synthesis are shown in Table S1.

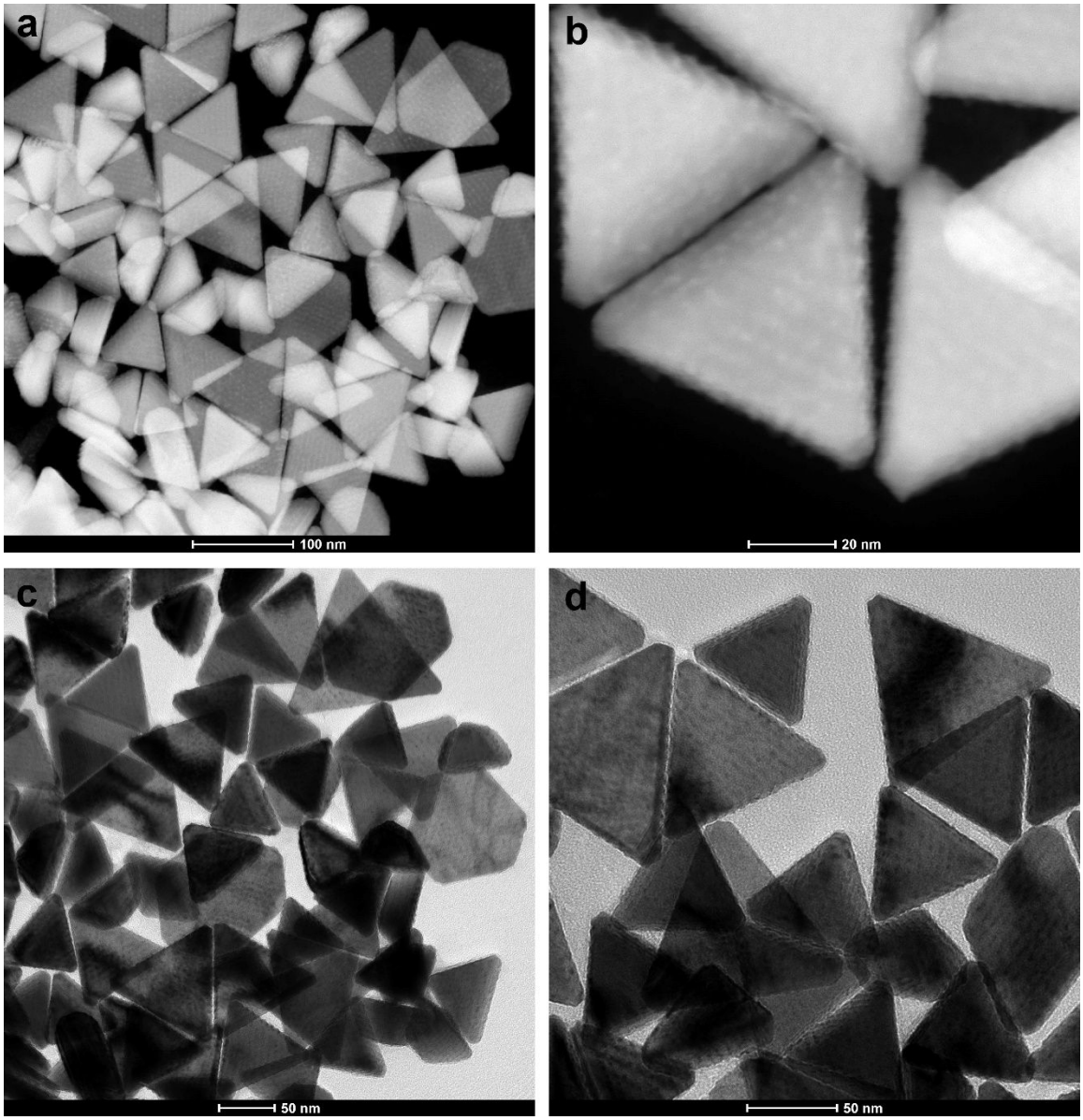


**Figure S5.** Morphology of Au NT-Pt. (a, b) STEM image of Au NT-Pt NPs, (c, d) TEM image of Au NT-Pt NPs.

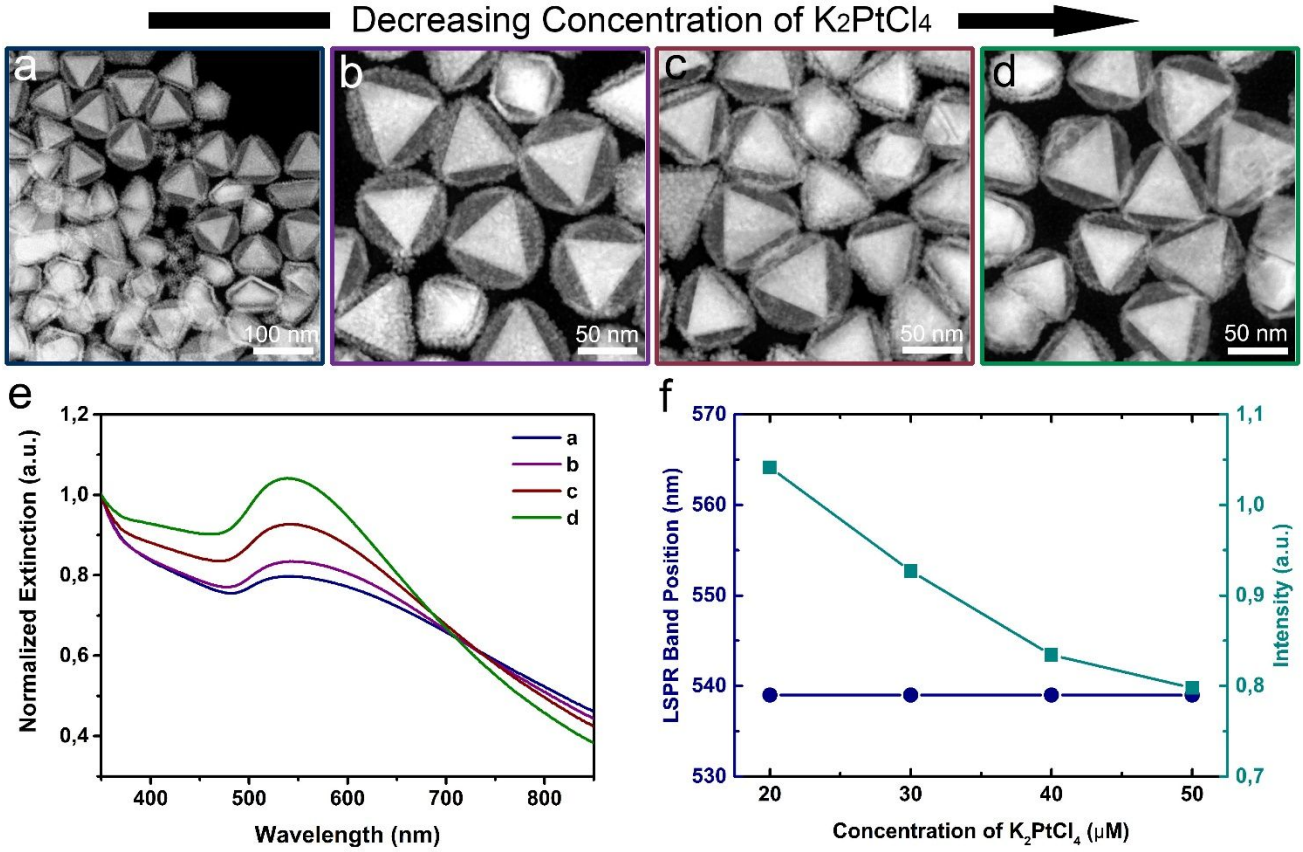


**Figure S6.** Morphological evolution of Au NT-AgPt NPs synthesized with various concentrations of $K_2PtCl_4$. STEM-HAADF images indicated Au NTAgPt NPs obtained as the concentration of $K_2PtCl_4$ was: a) 50 μM, b) 40 μM, c) 30 μM, and d) 20 μM. e) UV-Vis spectra and f) LSPR band position of Au NT-AgPt NPs showed in a-d. More details of the synthesis are shown in Table S1.

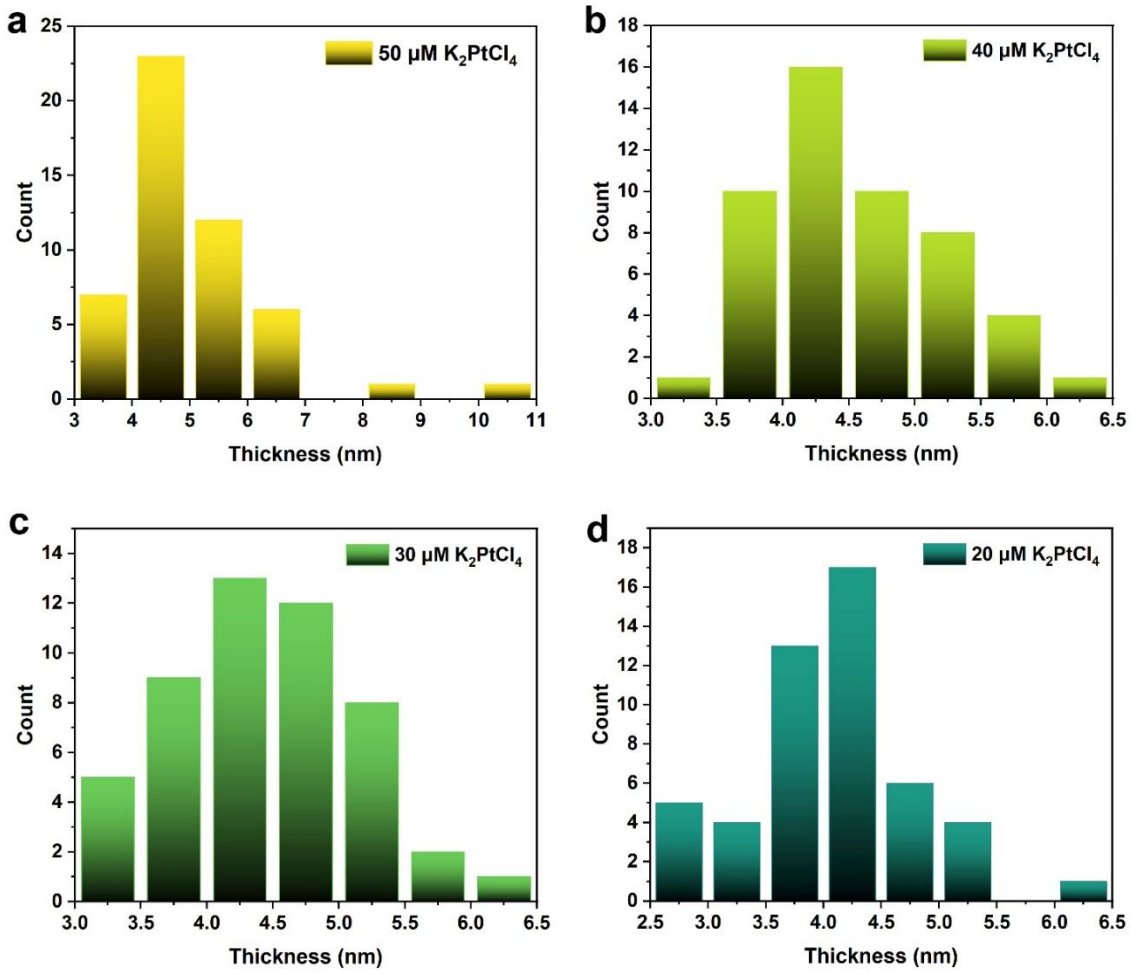


**Figure S7.** The AgPt shell thickness of Au NT-AgPt NPs synthesized with various concentrations of $K_2PtCl_4$. Histogram of Ag-Pt shell thickness distributions. The Ag-Pt shell thickness in above Figure was: (a) 5.1±1.2 nm, (b) 4.5±0.7 nm, (c) 4.4±0.7 nm, (d) 4±0.7 nm. Corresponding morphologies are showed in Figure S6.

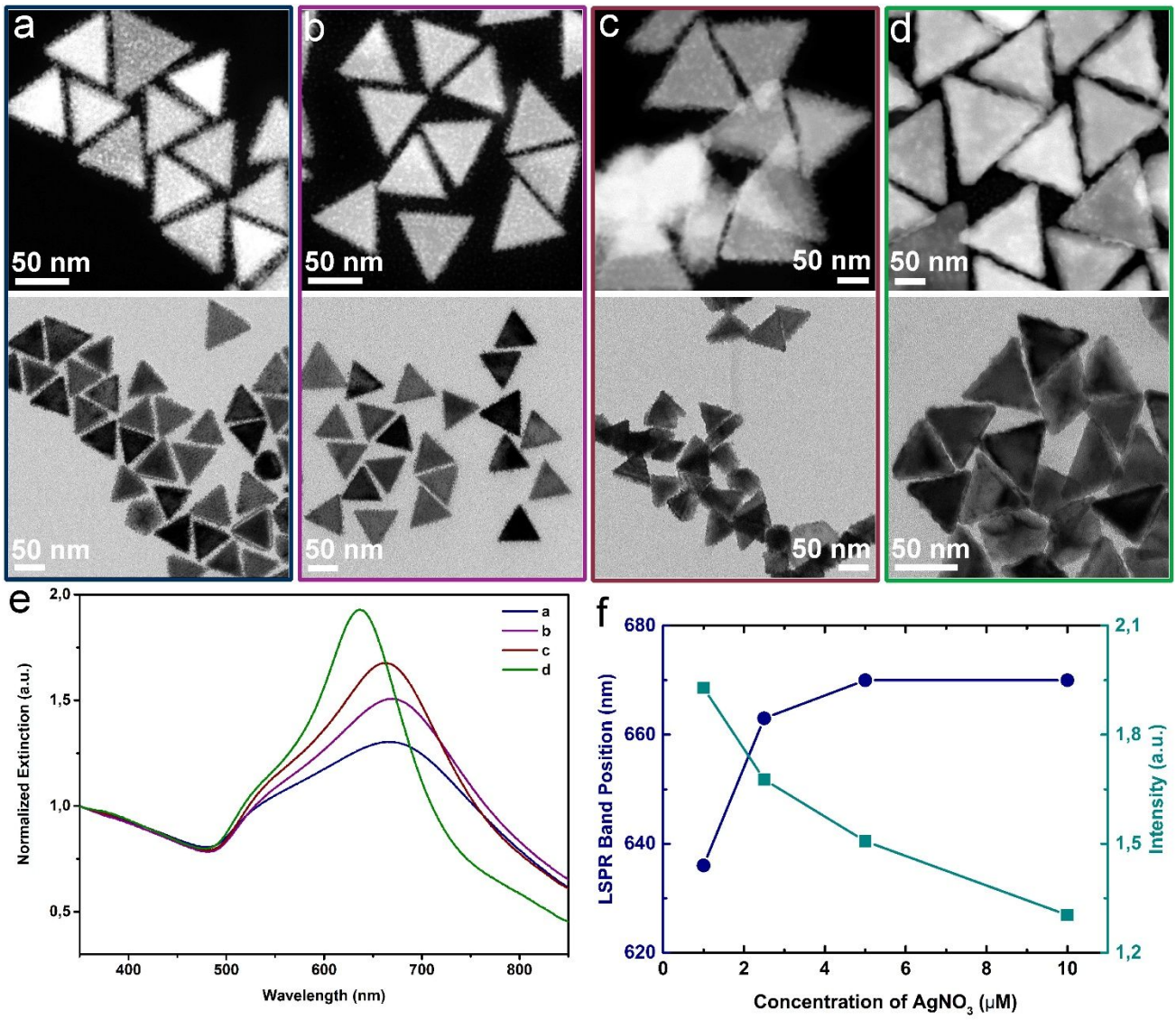


**Figure S8.** Morphological evolution of Au NT-AgPt NPs for various concentrations of $AgNO_3$. STEM-HAADF (up) and TEM (down) images indicated Au NT-AgPt NPs acquired as the concentration of $AgNO_3$ in the growth solution was: a) 20 μM, b) 15 μM, c) 10 μM, and d) 5 μM. e) UV-Vis spectra and f) LSPR band position of Au NT-AgPt NPs showed in a-d. More details of the synthesis are shown in Table S1.

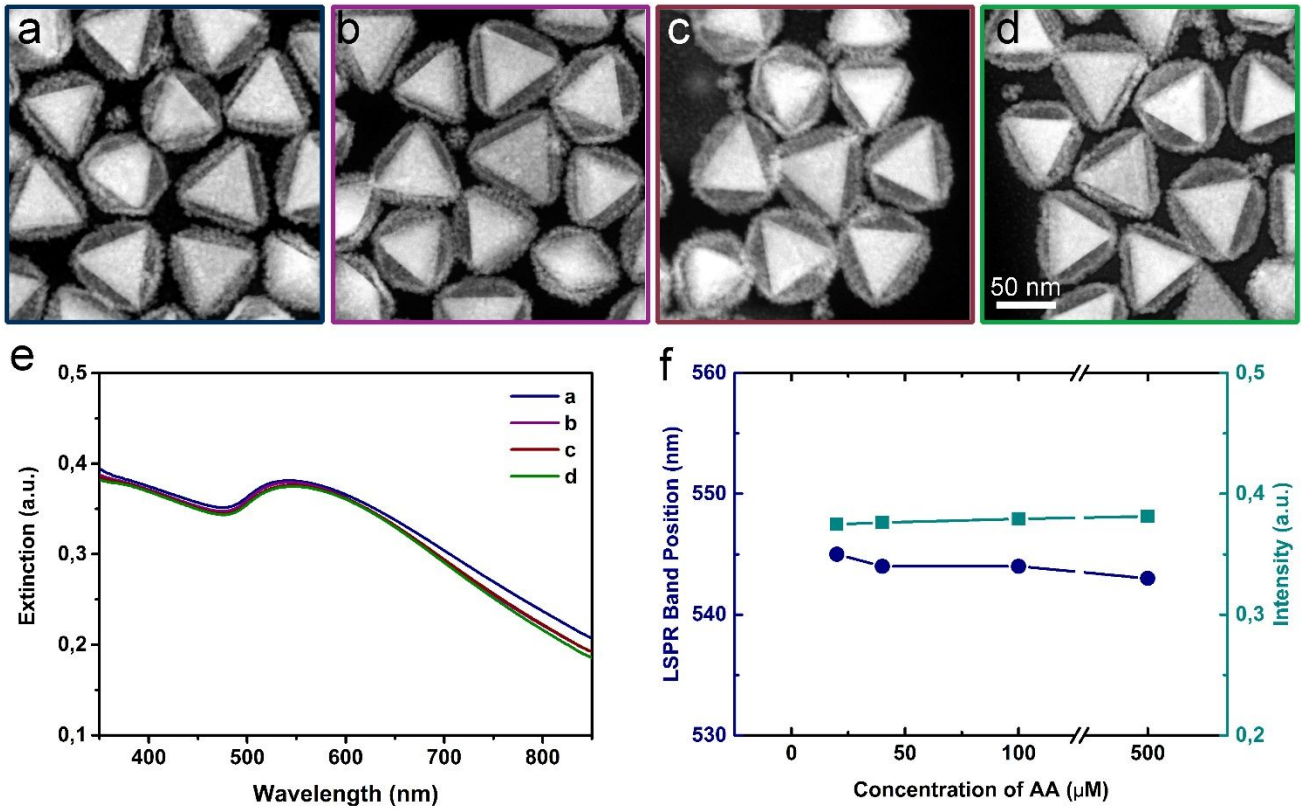


**Figure S9.** Morphological evolution of Au NT-AgPt NPs synthesized with various concentrations of AA. STEM-HAADF of NPs acquired as the concentration of AA was: (a) 5.00 mM, (b) 1.00 mM, (c) 0.40 mM, and (d) 0.20 mM. (e) UV-Vis spectra and f) LSPR band position of Au NT-AgPt NPs showed in a-d. More details of the synthesis are shown in Table S1.

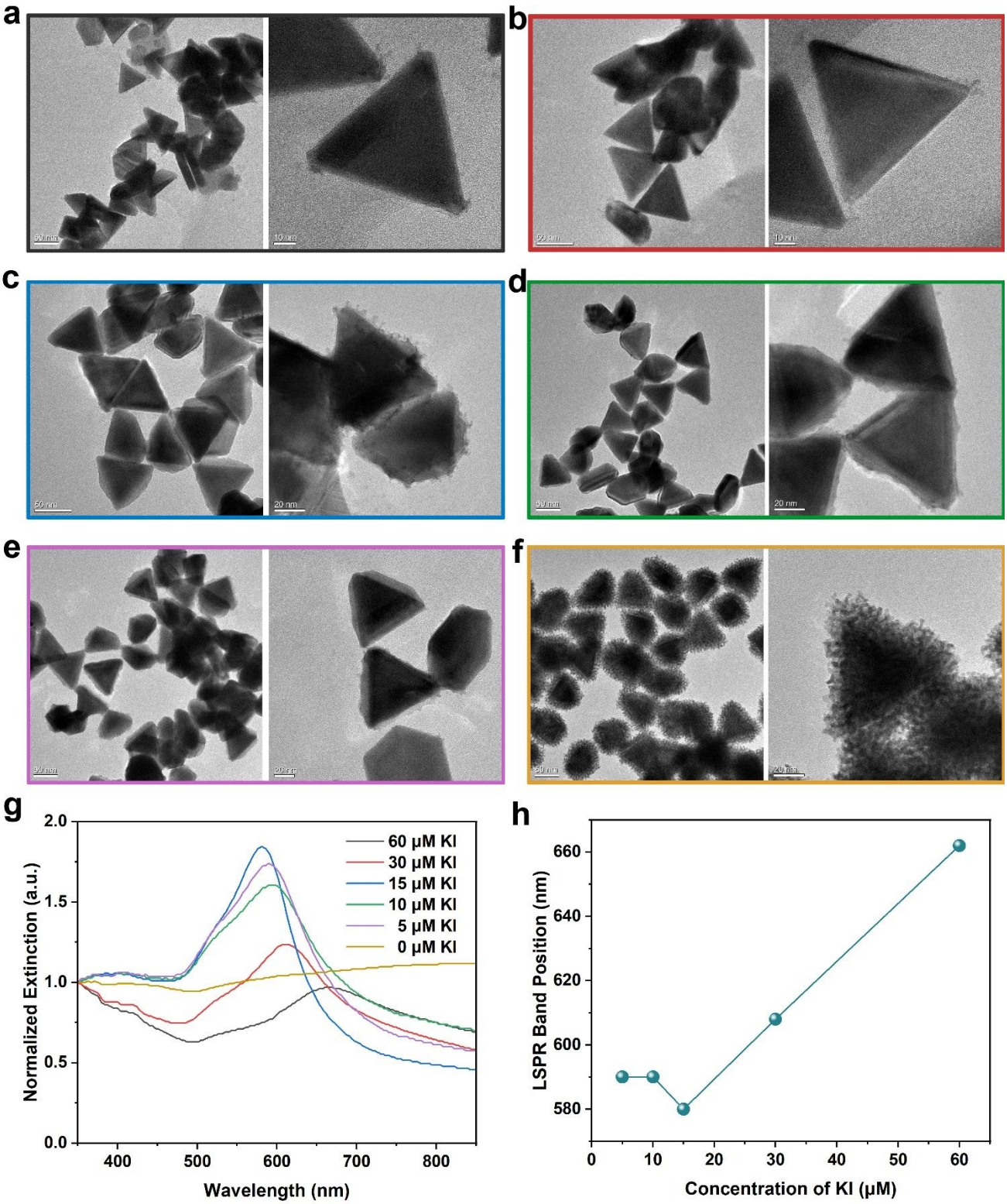


**Figure S10.** Morphological evolution of Au NT-AgPt NPs synthesized with various concentrations of KI. TEM images of NPs acquired as the concentration of KI was: (a) 60 μM, (b) 30 μM, (c) 15 μM, (d) 10 μM, (e) 5 μM, and (f) 0 μM. (g) UV-Vis spectra and (h) LSPR band position of Au NT-AgPt NPs showed in (a-f). More details of the synthesis are shown in Table S2.

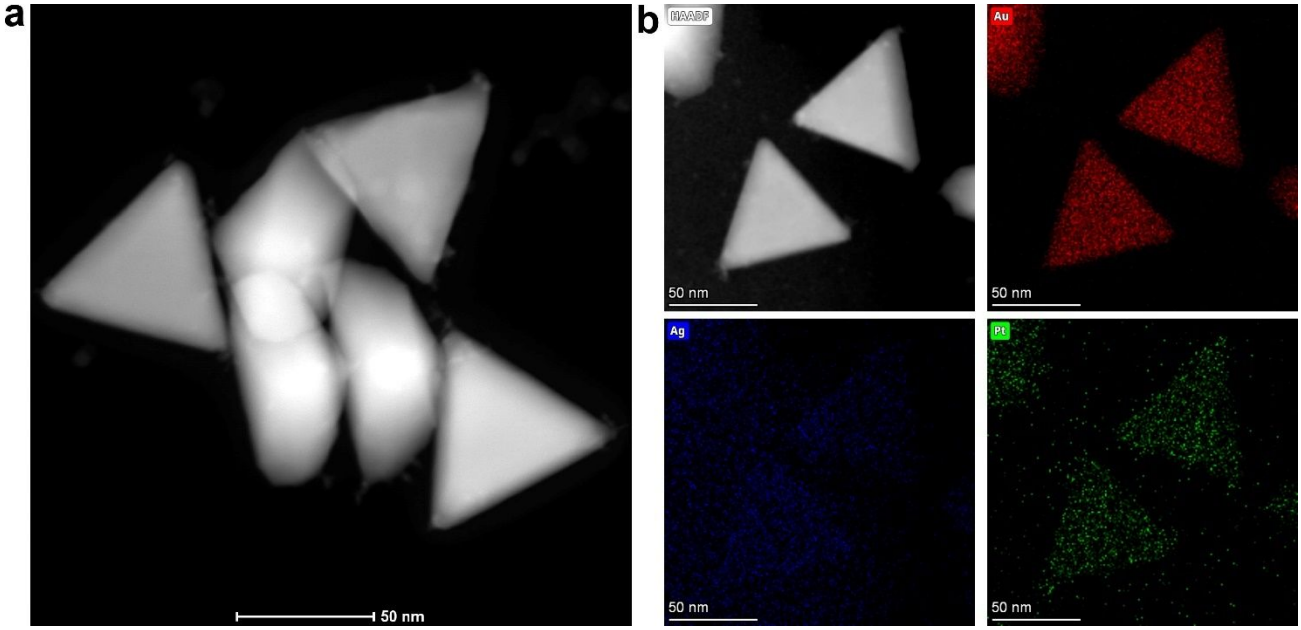


**Figure S11.** (a) STEM-HAADF image and (b)STEM-EDS elemental maps of Au NT-AgPt site-selective growth NPs which acquired as the concentration of KI was 60 μM.

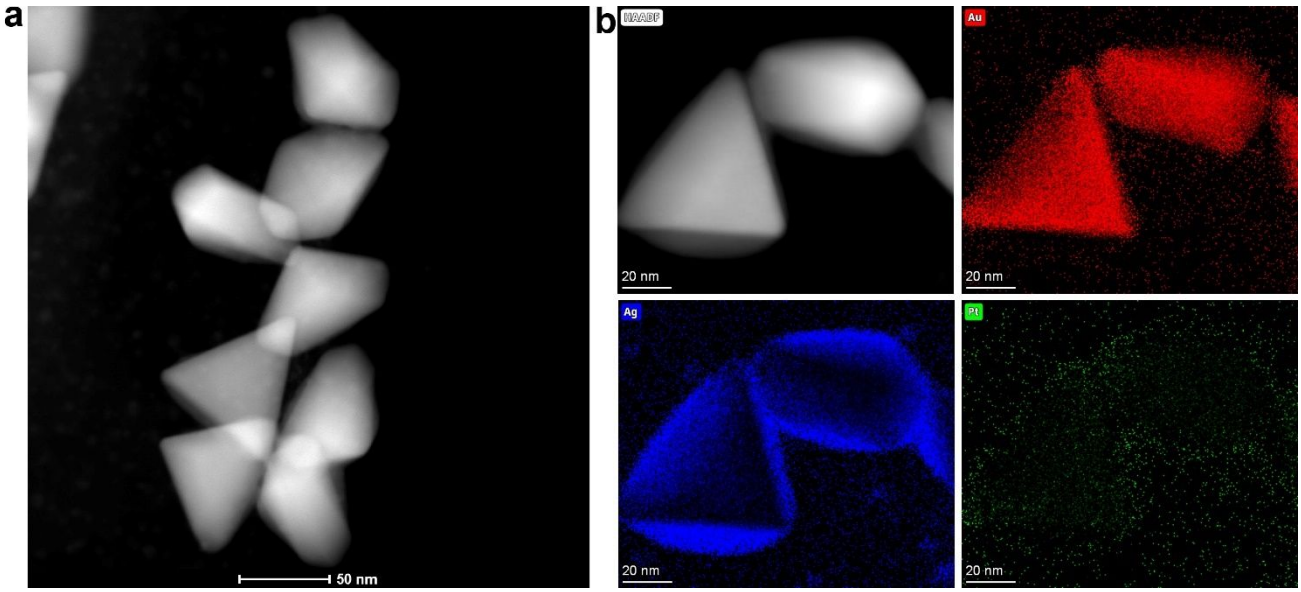


**Figure S12.** (a) STEM-HAADF image and (b) STEM-EDS elemental maps of Au NT-AgPt NPs which acquired as the concentration of KI was 15 μM.

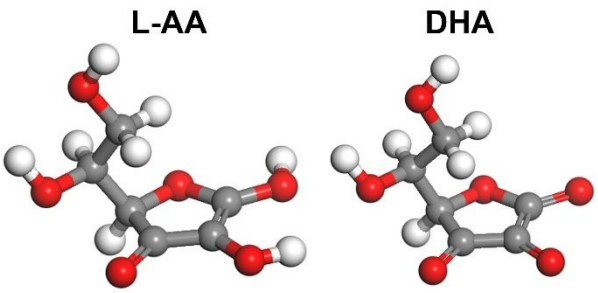


**Figure S13.** Molecule structure of $C_6H_8O_6$ (L-AA) and $C_6H_6O_6$ (DHA).

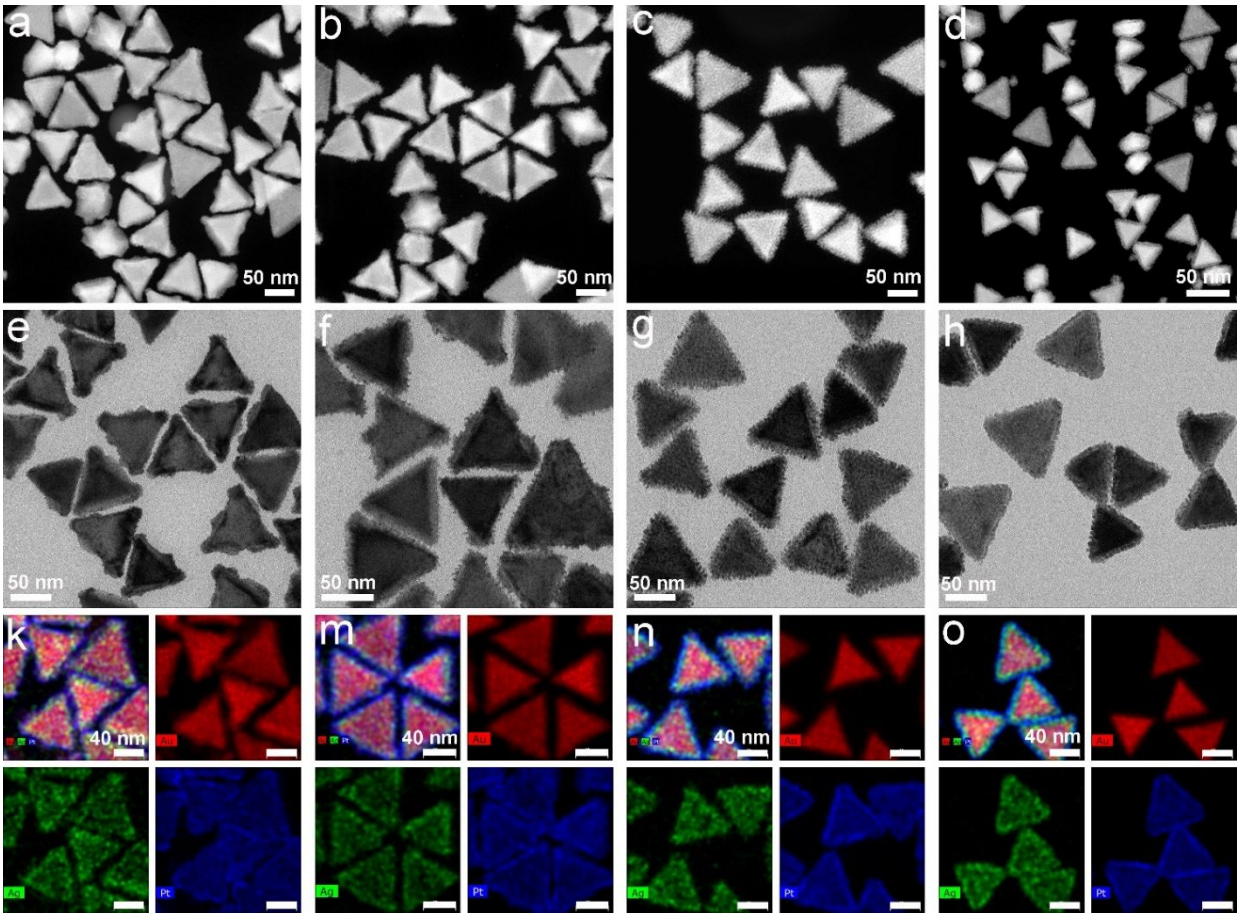


**Figure S14.** Morphological evolution of Au NT-AuAgPt NPs synthesized with various concentrations of Au and Ag. The concentration of $AgNO_3$ and $HAuCl_4$ ratios in the growth solution was: (a, e, k) $AgNO_3$ (20 μM)/ $HAuCl_4$ (40 μM), (b, f, m) $AgNO_3$ (30 μM)/ $HAuCl_4$ (30 μM), (c, g, n) $AgNO_3$ (40 μM)/ $HAuCl_4$ (20 μM), and (d, h, o) $AgNO_3$ (50 μM)/ $HAuCl_4$ (10 μM).The details of the synthesis are shown in Table S3. The scale bar indicates 50 nm in all STEM images and 40 nm in all STEM-EDS elemental maps.

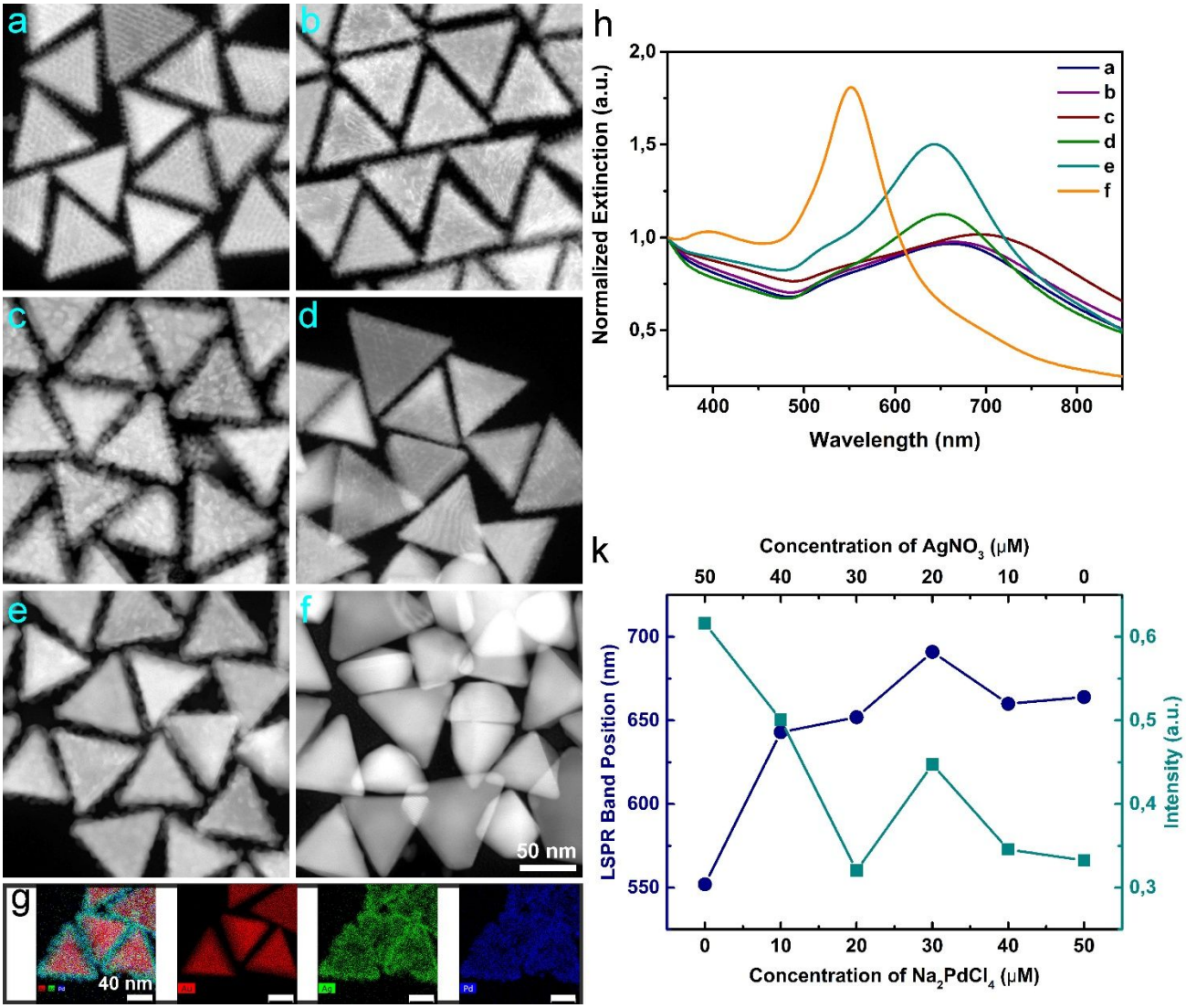


**Figure S15.** Shape evolution of Au NT-AgPd NPs synthesized while changing the ratio of Pd and Ag precursors. The concentration of $AgNO_3$ and $Na_2PdCl_4$ ratios in the growth solution was: (a) $AgNO_3$ (0 μM)/ $Na_2PdCl_4$ (50 μM), (b) $AgNO_3$ (10 μM)/ $Na_2PdCl_4$ (40 μM), (c, g) $AgNO_3$ (20 μM)/ $Na_2PdCl_4$ (30 μM), (d) $AgNO_3$ (30 μM)/ $Na_2PdCl_4$ (20 μM), (e) $AgNO_3$ (40 μM)/ $Na_2PdCl_4$ (10 μM), and (f) $AgNO_3$ (50 μM)/ $Na_2PdCl_4$ (0 μM).The details of the synthesis are shown in **Table S4**. The scale bar indicates 50 nm in all STEM images and 40 nm in the STEM-EDS elemental maps.

## References:


S1. O'Brien, M. N.; Jones, M. R.; Kohlstedt, K. L.; Schatz, G. C.; Mirkin, C. A., Uniform circular disks with synthetically tailorable diameters: two-dimensional nanoparticles for plasmonics. *Nano Lett.* **2015,** *15* (2), 1012-7.

S2. Johnson, P. B.; Christy, R. W., Optical Constants of the Noble Metals. *Phys. Rev. B* **1972,** *6* (12), 4370-4379.

S3. Fan, F.-R.; Liu, D.-Y.; Wu, Y.-F.; Duan, S.; Xie, Z.-X.; Jiang, Z.-Y.; Tian, Z.-Q., Epitaxial Growth of Heterogeneous Metal Nanocrystals: From Gold Nano-octahedra to Palladium and Silver Nanocubes. *J. Am. Chem. Soc.* **2008,** *130*, 6949–6951.

S4. Bauer, E.; van der Merwe, J. H., Structure and growth of crystalline superlattices: From monolayer to superlattice. *Phys. Rev. B Condens. Matter.* **1986,** *33* (6), 3657-3671.

S5. Xia, Y.; Xia, X.; Peng, H. C., Shape-Controlled Synthesis of Colloidal Metal Nanocrystals: Thermodynamic versus Kinetic Products. *J. Am. Chem. Soc.* **2015,** *137* (25), 7947-66.